J Appl Electrochem (2010) 40:1817–1827
DOI 10.1007/s10800-010-0139-1

ORIGINAL PAPER

On the activation and physical degradation of boron-doped diamond surfaces brought on by cathodic pretreatments

Giancarlo R. Salazar-Banda · Adriana E. de Carvalho · Leonardo S. Andrade · Romeu C. Rocha-Filho · Luis A. Avaca

Received: 14 January 2010 / Accepted: 14 April 2010 / Published online: 18 May 2010
© Springer Science+Business Media B.V. 2010

Abstract The electrochemical activation and physical degradation of boron-doped diamond (BDD) electrodes with different boron doping levels after repeated cathodic pretreatments are reported. Galvanostatic cathodic pretreatment passing up to -14000 C cm^{-2} in steps of -600 C cm^{-2} using -1 A cm^{-2} caused significant physical degradation of the BDD surface, with film detachment in some areas. Because of this degradation, a great increase in the electrochemically active area was observed in Tafel plots for the hydrogen evolution reaction (HER) in acid media. The minimum cathodic pretreatment needed for the electrochemical activation of the BDD electrodes without producing any observable physical degradation on the BDD surfaces was determined using electrochemical impedance spectroscopy (EIS) measurements and cyclic voltammetry: -9 C cm^{-2}, passed at -1 A cm^{-2}. This optimized cathodic pretreatment can be safely used when electrochemical experiments are carried out on BDD electrodes with doping levels in the range between 800 and 8000 ppm.

Keywords Boron-doped diamond electrodes · Cathodic pretreatment · Surface erosion · Surface activation · Electrochemical impedance spectroscopy

G. R. Salazar-Banda · L. A. Avaca (✉)
Instituto de Química de São Carlos, Universidade de São Paulo, C.P. 780, São Carlos, SP 13560-970, Brazil
e-mail: avaca@iqsc.usp.br

A. E. de Carvalho · L. S. Andrade · R. C. Rocha-Filho
Departamento de Química, Universidade Federal de São Carlos, C.P. 676, São Carlos, SP 13560-970, Brazil

G. R. Salazar-Banda
Instituto de Tecnologia e Pesquisa/Programa de Pós-Graduação em Engenharia de Processos, Universidade Tiradentes, Aracaju, SE 49032-490, Brazil

A. E. de Carvalho
Departamento de Química, Universidade Federal de Mato Grosso do Sul, Av. Senador Filinto Müller 1555, Campo Grande, MS 79074-460, Brazil

L. S. Andrade
Departamento de Química, Universidade Federal de Goiás, Campus de Catalão, Avenida Lamartine P. Avelar 1120, Catalão, GO 75704-020, Brazil

1 Introduction

The electrochemical behaviour of boron-doped diamond (BDD) electrodes depends on their physical, chemical, and electronic properties. These properties are especially affected by the surface termination (hydrogen, oxygen, and others). In this sense, Suffredini et al. [1] studied the effect of surface electrochemical pretreatments on the electrochemical response of the $Fe(CN)_6^{4-/3-}$ redox couple on BDD electrodes. This couple presented a reversible behaviour on cathodically pretreated BDD electrodes and a quasi-reversible one after anodic pretreatment. Moreover, using electrochemical impedance spectroscopy (EIS) it was observed that the resistance associated to a high-frequency element presented values of over 300 or 4 Ω cm^2 after anodic or cathodic pretreatments, respectively. Mahe et al. [2] also used anodic and cathodic pretreatments to study the electrochemical reactivity of the $Fe(CN)_6^{4-/3-}$ system on BDD electrodes and observed that the cathodic pretreatment renders a great reproducibility and a very high rate for the electron transfer. Previously, Holt et al. [3] studied the reduction on BDD electrodes of tetrachloroaurate(III) dissolved in dilute aqua regia and, among other

things, investigated the effect of electrochemical surface pretreatments. They concluded that cathodic pretreatments of the BDD surface considerably increase the rate for both the deposition and stripping of gold; additionally, they reported that the effect of the surface pretreatment remained even after the electrode was exposed to the laboratory atmosphere for several days.

In a more recent investigation from our laboratories [4] it was shown that cathodically pretreated BDD surfaces exhibit a dynamic electrochemical behaviour, i.e. a loss of the reversibility for the redox couple $Fe(CN)_6^{4-/3-}$ as a function of time, but at a rate inversely dependent on the boron doping level. This phenomenon was associated to a loss of superficial hydrogen due to oxidation by oxygen from the air. Therefore, these results strongly suggest that cathodic pretreatments should be performed just before the electrochemical experiments in order to ensure reliable and reproducible results.

Cathodic pretreatments have also been found to be a simple and very efficient procedure to improve the electrochemical activity of BDD surfaces. The use of this type of pretreatment allows achieving very low detection and quantification limits and high data reproducibility for the analysis of several substances in aqueous solutions [5–18]. The pretreatment procedure commonly used consists in either a 30 min potentiostatic polarization at −3.0 V versus the hydrogen electrode in the same solution (HESS) [1–9, 11, 14] or a galvanostatic polarization (at least −0.5 A cm^{-2} for at least 60 s) [10, 12, 13, 15–18]. Such polarizations produce intense hydrogen evolution, which can be accompanied by an undesirable increase in the solution temperature depending on the total charge passed. Additionally, several publications have reported the use of diamond electrodes as very efficient cathode materials for the electrochemical reduction of nitrate ions dissolved in high concentrations in wastewaters [19–22]. As the nitrate reduction takes place at fairly negative potentials where the hydrogen evolution reaction (HER) also occurs, the efficiency of the process might be related to surface activation.

More recently, further experiments carried out in our laboratories revealed that repeated cathodic polarizations might physically degrade the BDD electrode surface. Deuerler et al. [23] studied the adhesion and wear behaviour of micro- and nanostructured crystalline diamond films by a cavitation test, using the ultrasonic technique to stimulate their degradation. These authors showed that diamond surfaces might be effectively eroded under those conditions. In fact, for a microstructured diamond film of 3 μm thickness, they observed that approximately 9% of surface damage was reached after cavitation charging for 35 ks. Nanocrystalline diamond thin films deposited on a silicon substrate were also tested using cavitation erosion experiments and the eroded surfaces examined by scanning electron microscopy (SEM) [24]. In this case, after 30 min of experiment the formation of micrometer-sized pits was visible; after 90 min, these pits propagated across the film surface producing large pores, whereas after 150 min most of the film was removed from the silicon substrate. The authors concluded that cavitation erosion resistance is inversely proportional to the roughness of the diamond film, which is in agreement with the findings by Deuerler et al. [23] that nanocrystalline films are more resistant to cavitation erosion.

Additionally, in 1998, Katsuki et al. [25] reported that BDD electrodes were gradually corroded under high anodic polarization (2 A cm^{-2} at 60 °C) in 10% (vol.) H_2SO_4; however, the BDD resistance to corrosion increased with its doping level. More recently, Panizza et al. [26] showed that, while in 1 mol L^{-1} H_2SO_4 no appreciable polishing of the BDD surface is observed, even after 256 h of polarization using 1 A cm^{-2} at 40 °C, the BDD morphology is changed in a few hours if 3 mol L^{-1} acetic acid is added to the 1 mol L^{-1} H_2SO_4 solution. Similarly, Duo et al. [27] reported significant changes in the BDD surface morphology after severe anodic polarization (1 A cm^{-2}) in 1 mol L^{-1} $HClO_4$. However, to the best of our knowledge there are no reports in the literature regarding the physical degradation of BDD surfaces produced by cathodic polarizations.

On the other hand, Holt et al. [28] measured the pattern of conductivity and electrochemical activity at surfaces of hydrogen-terminated BDD electrodes, with low boron doping levels, using conductive probe atomic force microscopy (CP-AFM) and scanning electrochemical microscopy (SECM). With the CP-AFM measurements these authors showed that the BDD surface is predominantly insulating, with discrete conducting areas, randomly and not uniformly distributed on the surface. With SECM imaging they correlated these conductive areas (predominantly located at grain boundaries) with the electrochemical activity of the electrode (surface partially electrochemically active) and showed that the active area of the electrodes increased with the boron doping level. Prior to that, Becker and Jüttner [29–31] concluded that the electrochemical behaviour of the $Fe(CN)_6^{4-/3-}$ redox couple was due to a partial blocking of the BDD electrode surface with reversible charge transfer at active sites.

Additionally, Wilson et al. [32] used the CP-AFM, SECM and cathode-luminescence (CL) techniques to investigate the electrochemical behaviour of oxygen-terminated highly doped polycrystalline BDD. With CL imaging they demonstrated that boron uptake was non-uniform across the BDD surface, with an impact on the local conductivity as seen through CP-AFM. While with CP-AFM no evidence for enhanced grain boundary conductivity was found, two significantly different

conductivity domains were found. With the use of SECM, local heterogeneities were also observed in the electroactivity of the BDD surface, consistent with the two different conductivity domains. Szunerits et al. [33], using micro-Raman spectroscopy and Raman imaging, Kelvin probe force microscopy, CP-AFM, and SECM, reported similar results about the non-uniform boron uptake across the surface of highly doped BDD electrodes. Two different conductivity domains were also evidenced, corresponding to either metallic or semiconducting properties. Nevertheless, all these approaches did not reveal the occurrence of enhanced doping or boron depletion at the grain boundaries. However, electrochemical studies regarding the relationship between the doping level and the electrochemical active sites of BDD electrodes are needed and therefore these concerns are further investigated hereinafter.

Considering the very promising cathodic applications of BDD electrodes and the importance of cathodic pretreatments to ensure the sensitivity, reliability, and reproducibility of many electroanalytical results, the aim of this study is to investigate the activation and physical degradation of BDD surfaces after repeated cathodic polarizations. For that, SEM, AFM, and electrochemical techniques are used. To avoid any undesired degradation of the surface, the minimum (optimum) charge density to be passed in the cathodic pretreatment to ensure high electrochemical activity of the BDD surfaces is determined, based on cyclic voltammetry and EIS data.

2 Experimental

The BDD films were prepared on silicon wafers at the Centre Suisse d'Electronique et de Microtechnique SA (CSEM), Neuchâtel, Switzerland, using the hot filament chemical vapor deposition (HF-CVD) technique; further details are given elsewhere [4]. The final boron content of the different electrodes used as 1.2 cm × 1.2 cm plates was of the order of 800, 2000, and 8000 ppm. Some comparative experiments were also carried out using a 300 ppm BDD sample.

The electrochemical experiments were carried out using a model PGSTAT 30 Autolab potentiostat/galvanostat and a two-compartment Pyrex® glass cell provided with three electrodes and degassing facilities for bubbling N_2. The reference electrode was a HESS prepared just before measurements and all potentials are referred to this system. The auxiliary electrode was a 2 cm^2 Pt foil. Working electrodes were clamped in firm contact at the side of the cell by means of a rubber O-ring leaving an exposed area of the BDD plate of 0.63 cm^2. Prior to use, the BDD electrode surface was cleaned with ethanol and rinsed with ultrapure water. All reagents were Merck P.A. and the water was purified by a Milli-Q system from Millipore. Prior to measurements, the cell solution was deaerated by bubbling N_2 for 10 min. The supporting electrolyte used for the pretreatments and in the electrochemical experiments was a 0.5 mol L^{-1} H_2SO_4 aqueous solution.

As-received (fresh) samples of the BDD electrodes were initially subjected to steps of cathodic pretreatment. Some steps were potentiostatic polarizations at −3.0 V for 30 min (corresponding to a passed charge density of about −600 C cm^{-2} in the first polarization) and other steps were galvanostatic polarizations up to −600 C cm^{-2}. Meanwhile, to determine the minimum necessary charge density for the cathodic pretreatment, different charge densities were passed using −1 A cm^{-2}. Before each cathodic pretreatment, a 5 C cm^{-2} anodic pretreatment was carried out using 1 A cm^{-2}. The electrical properties of as-received or pretreated BDD electrodes were investigated by EIS, in the presence of a 1.0 mmol L^{-1} $K_4[Fe(CN)_6]$ acid solution, applying the equilibrium potential with an ac perturbation of 5 mV (rms), from 10 MHz to 100 kHz. Likewise, the reversibility of the $Fe(CN)_6^{4-/3-}$ redox couple was assessed by cyclic voltammetry in the same electrolyte.

SEM measurements were carried out in a Leica Cambridge scanning electron microscope (Stereoscan 440 model) with a silicon–lithium detector and a Be window, applying 113 eV. The surface topology studies by AFM were carried out in a TopoMetrix® AFM Explorer.

3 Results and discussion

It is important to mention that the different pretreatments performed on the BDD electrodes were carried out in steps due to the intense increase of the solution temperature as a result of the circulating current (Joule effect). For instance, the temperature reached ∼60 °C after a 30 min polarization at −3.0 V using a two-compartment cell (60 mL) and two 800 ppm BDD electrodes as anode and cathode.

Figure 1a, b, and c shows AFM images for an 800 ppm BDD electrode after a 30 min pretreatment at −3.0 V (approx. −600 C cm^{-2}), a 180 min pretreatment at −3.0 V (approx. −6000 C cm^{-2}), and a galvanostatic pretreatment (−1 A cm^{-2}) in steps of −600 C cm^{-2} until −14000 C cm^{-2} was reached, respectively. As it can be observed, Fig. 1a shows the uniform topography of the BDD surface, while its SEM micrograph recorded at 40000× (Fig. 1d) shows in detail the well-known [26, 34] regular pyramidal structure of BDD surfaces. In fact, this morphology of the surface is very similar to the AFM and SEM images obtained on as-received BDD electrodes (not shown). Consequently, no apparent BDD surface degradation was observed after this time (30 min) of cathodic pretreatment.

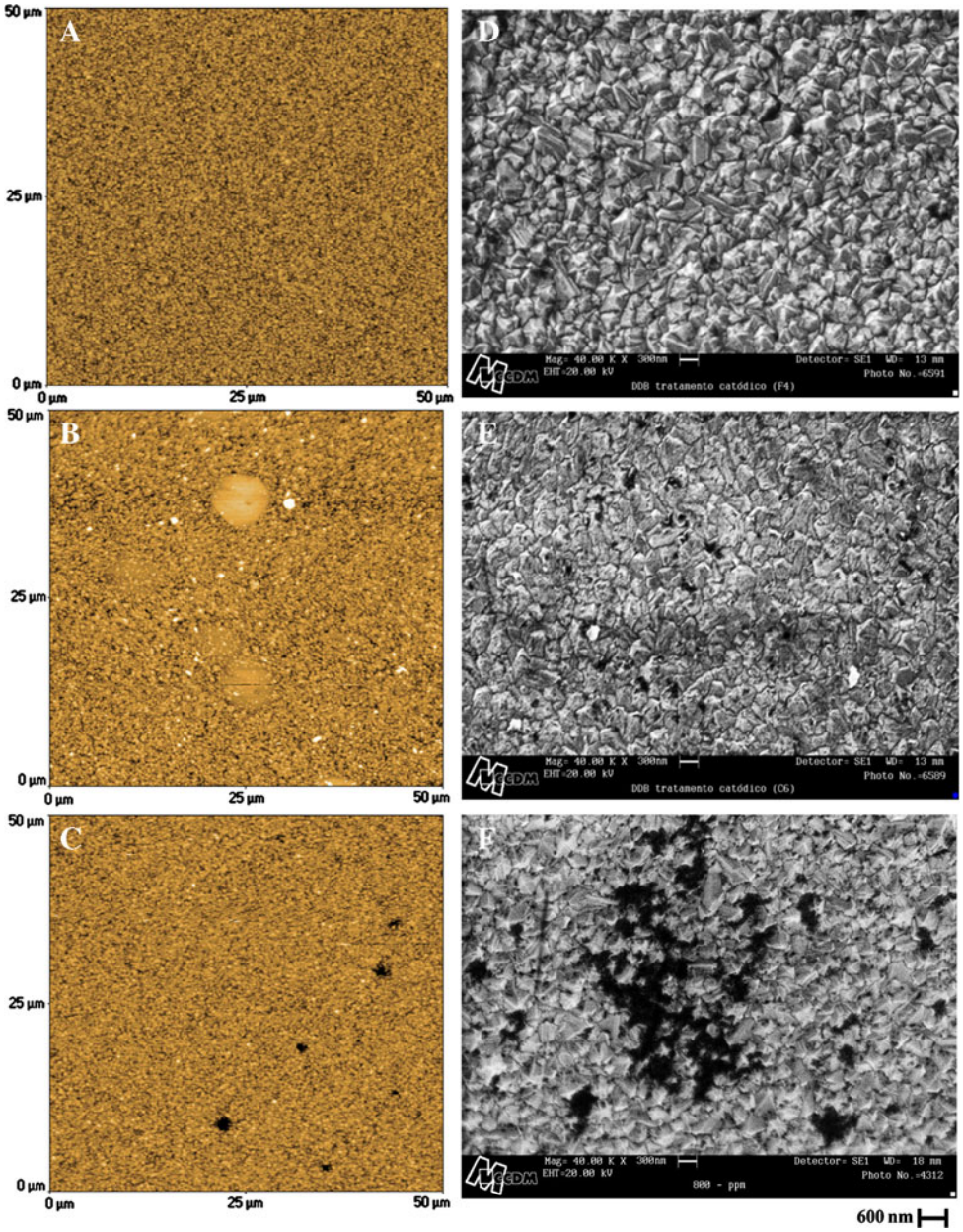

Fig. 1 **a–c** AFM 2D topography images recorded in a 50 µm × 50 µm area and **d–f** 40000× SEM images of an 800 ppm BDD electrode surface, after the following cathodic pretreatments: **a**, **d** 30 min at −3.0 V (approx. −600 C cm^{-2}), **b**, **e** 180 min at −3.0 V (approx. −6000 C cm^{-2}), **c**, **d** extended galvanostatic pretreatment in steps of −600 C cm^{-2} using −1 A cm^{-2} until a charge density of −14000 C cm^{-2} was passed

Meanwhile, a smoothing of the BDD surface is clearly observed after the 180 min potentiostatic pretreatment approx. −6000 C cm^{-2}), carried out applying six polarization steps in intervals of 30 min each (Fig. 1b, e); some small cavities (about 100 nm wide) can already be observed in the micrograph of Fig. 1e. As a consequence, the maximum peak-to-valley distance obtained from the AFM image (Fig. 1b) increased 44% in relation to that of Fig. 1a; this is a demonstration that the BDD surface topology was modified after 180 min of cathodic pretreatment. It is worthwhile mentioning that a 30 min pretreatment (data not shown) caused an increase of about 2% in the maximum peak-to-valley distance relative to the as-received surface. Likewise, after being galvanostatically (−1 A cm^{-2}) pretreated by passing −6000 C cm^{-2} (data not shown), the BDD surface presented a surface degradation similar to those observed in the potentiostatically pretreated BDD sample (Fig. 1b, e).

In addition, extending the galvanostatic polarization in steps of −600 C cm^{-2} at −1 A cm^{-2} until −14000 C cm^{-2} were passed resulted in a significant physical degradation of the BDD surface (Fig. 1c); cavities are now visible on the BDD surface and the maximum peak-to-valley distance is 51% higher than the one observed on an as-received BDD

electrode. The SEM micrograph obtained at high magnification for this electrode (Fig. 1f) shows the extent of this surface degradation, with clear disappearance of patches of the BDD film that leads to voids. Something similar was previously reported by Duo et al. [27], but caused by severe anodic polarization in $HClO_4$. Exposures of the substrate surface as the one seen in Fig. 1f were also observed in erosion studies of diamond coatings [24, 35]. Therefore, the substantial degradation of the BDD surface shown in Fig. 1c and f brought about by the long cathodic pretreatment may have been exacerbated by the consequent increase of the temperature, analogous to what occurred in cavitation erosion tests [23]. Similar surface degradations are also found for 2000 and 8000 ppm BDD electrodes after the same cathodic pretreatments.

Taking into account the here reported superficial degradation phenomenon caused by the cathodic pretreatments, it can be assumed that the changes in the morphology of the BDD surface are due mainly to an erosion process associated to the very intense hydrogen evolution: most probably atomic hydrogen diffuses into interstices or imperfections in the electrode surface, thus causing its degradation. It is well known that hydrogen entry into metals or alloys may result in a degradation of the mechanical properties of those materials [36, 37]. The electrolytic deposition of hydrogen can sustain a fairly high equivalent pressure of hydrogen gas at a metal surface, where atomic hydrogen is initially contained in interstitial sites of the metal lattice [38]. Cathodic polarization produces hydrogen damage such as blisters, microcracks, and dislocations [39] due to the expansion of high-pressure hydrogen bubbles [40].

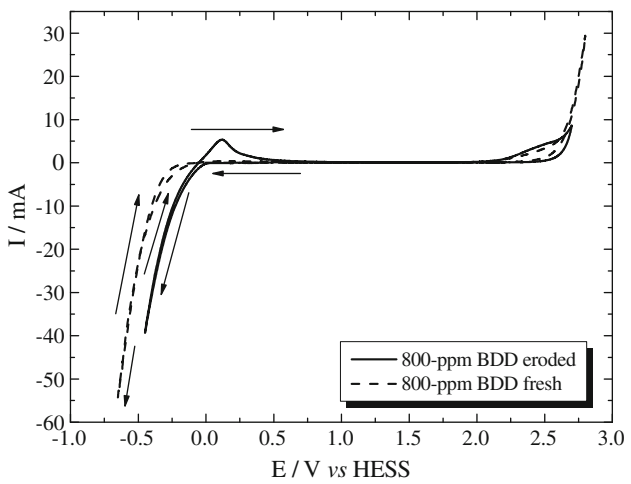

Fig. 2 Potential windows for eroded (*solid line*) and as-prepared (fresh; *dashed line*) 800 ppm BDD electrodes recorded at $v = 0.1$ V s^{-1} in a 0.5 mol L^{-1} H_2SO_4 aqueous solution. The scans were started at 0.0 V towards the cathodic direction

A clear indication of the formation of microcavities and/or microcracks in the BDD surface is observed in Fig. 2, where the electrochemical potential windows in acid media of fresh and cathodically pretreated (passing of -14000 C cm^{-2}) 800 ppm BDD electrodes are compared. The voltammogram of the eroded electrode (from now, this severely pretreated electrode will be designated as 'eroded 800 ppm BDD') displays a broad peak in the anodic scan (starting at about 0 V) that can be ascribed to hydrogen oxidation associated to a slow desorption process of atomic hydrogen from the superficial microvoids or microcracks produced in the BDD surface. In contrast, the voltammogram for the fresh 800 ppm BDD electrode does not show any anodic peak since its surface is regular and free of microvoids or microcracks.

On the other hand, an increase in the current density (based on the geometric area) was observed during potentiostatic cathodic pretreatments of the BDD electrodes. Figure 3a shows some chronoamperograms recorded during successive cathodic polarizations (at -3.0 V for 30 min) for the same 800 ppm BDD electrode surface. Due to the degradation of the surface during the polarizations, in other words, the formation of microvoids in the electrode surface, an apparent increase in the electrochemical active area is observed after each polarization step. Thus, the current density varies between -0.15 and -0.30 A cm^{-2} during the first polarization step, but reaches approx. -0.90 A cm^{-2} in the twelfth polarization step. Consequently, the absolute value of charge density passed changes from -600 C cm^{-2} during the first polarization step to -1500 C cm^{-2} during the twelfth polarization step (Fig. 3b).

In order to determine the effect of the physical degradation of the electrode surface on the electrochemical properties of BDD electrodes having different boron contents, steady-state polarization experiments were firstly performed with electrodes that had undergone a very mild cathodic pretreatment (-10 C cm^{-2} using -1 A cm^{-2}) and thus were not eroded. The corresponding Tafel plots for the HER in acid media are shown in Fig. 4. As it can be observed, the electrochemical response of the different electrodes greatly depends on the boron doping level. As a matter of fact, the current density values at similar electrode potentials are always larger for the electrodes with the higher doping level; thus, the 8000 ppm BDD electrode presents current densities almost three orders of magnitude higher than the one observed on the 800 ppm BDD electrode.

As the HER is a catalytic reaction that requires active sites available on the electrode surface for the initial adsorption of the hydrogen atom, it can be assumed that the increase in the current density values observed with the increase in the doping level is due to an increment in

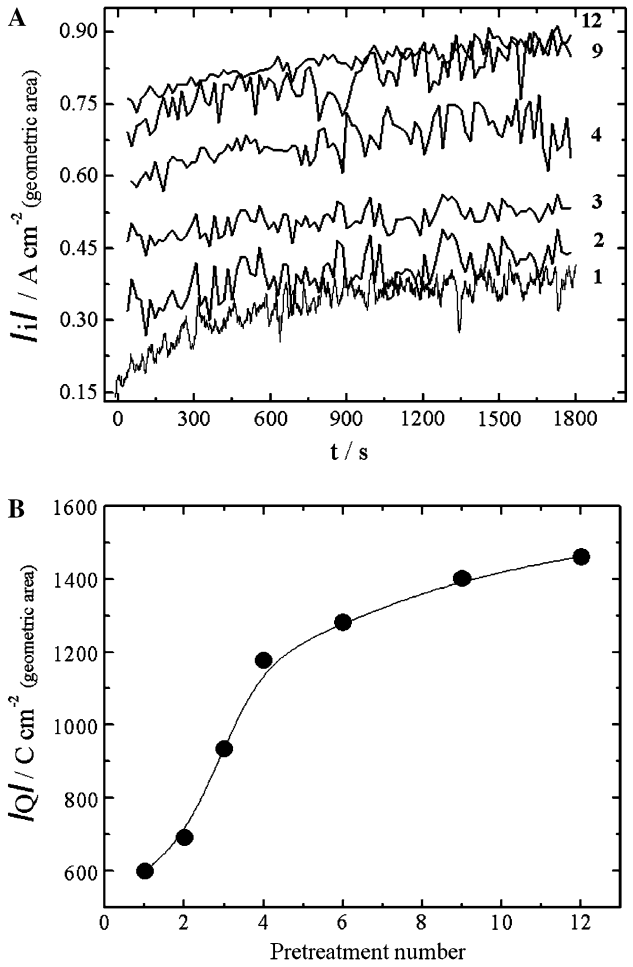

Fig. 3 **a** Examples of the chronoamperometric responses of an 800 ppm BDD electrode in a 0.5 mol L^{-1} H_2SO_4 solution, recorded at −3.0 V for twelfth consecutive 30 min pretreatment steps at that potential. **b** Charge density values during pretreatment steps (calculated using the geometric area of the electrode)

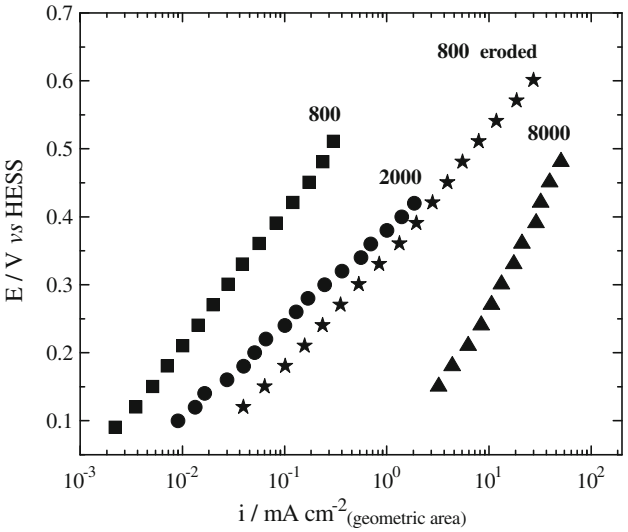

Fig. 4 Tafel plots for the HER recorded in a 0.5 mol L^{-1} H_2SO_4 aqueous solution on mildly cathodically pretreated (−10 C cm^{-2} at −1 A cm^{-2}) BDD electrodes with different doping levels (as indicated) and on an eroded 800 ppm electrode with the passage of −14000 C cm^{-2}

the number of active sites of the electrode surface, which is almost certainly directly associated to the superficial boron content. In this context, Suffredini et al. [41] studied the HER and the oxygen evolution reaction (OER) on a 4500–5000 ppm BDD electrode. They concluded that adsorption processes are responsible for the wide electrochemical window of the BDD electrode in aqueous medium. Interactions between water molecules and the electrode surface are strongly inhibited and the energies involved are, consequently, very high. The mechanisms for both the HER and OER have an initial adsorption step that is rate determining due to its extremely slowness on BDD surfaces. In addition, Cai [42] applied quantum mechanical theory and a local reaction centre model to the HER on Pt and on non-doped and BDD surfaces. From the obtained results, he concluded that non-doped diamond is a poor catalyst for the HER and attributed the observed catalytic reactivity for hydrogen evolution on BDD electrodes to the occurrence of weakly adsorbed hydrogen atoms that is made possible by the subsurface substitutional boron atoms. These results corroborate the relationship between the number of active sites and the doping level observed in Fig. 4.

On the other hand, Fig. 4 also shows that the eroded 800 ppm BDD electrode presents current densities higher than those obtained at a 2000 ppm BDD surface. In addition, the eroded 800 ppm BDD electrode shows an increase in the current density of about 150 times in comparison to the one only submitted to a very mild cathodic pretreatment. This enhancement in the current density clearly indicates an increase in the number of active (or conductive) sites for the HER brought on either by the severe pretreatment that exposes boron-rich sites or by a dramatic increase in the real surface area. It should be noticed that this behaviour was not observed for the redox couples most commonly used to investigate the electrochemical properties of BDD electrodes (e.g. $Fe(CN)_6^{4-/3-}$ and $Ru(NH_3)_6^{3+/2+}$). In those cases, the reactions are controlled by diffusion and are not sufficiently sensitive to active and/or blocked sites on the electrode surface that could act as microelectrode arrays, as demonstrated by Compton and co-workers [43–45]. In this sense, it should be recalled that Holt et al. [28] reported that a polycrystalline BDD thin film consists of highly conducting zones isolated from one another by more insulating regions; in other words, the electrical properties appear non-homogeneously across the BDD surface. Furthermore, they also reported that the fraction of the surface that is highly conducting increases with the boron doping level [28]. Hence, taking into account the results presented hereinbefore and those reported in the literature [23, 28],

the increase in the number of electrochemically active sites observed on the eroded 800 ppm BDD electrode (Fig. 4) can be understood if it is assumed that the surface degradation caused by the pretreatment somewhat exposes more boron to the diamond surface; consequently, an increase of the number of electrochemically active sites on the BDD surface could be expected.

Another important feature studied here was related to the relationship between the electrochemical potential window in acid media and the boron doping level of BDD electrodes. Figure 5 clearly shows that the width of this potential window is inversely dependent on the doping level. The observed values for the potential windows (for ±0.3 mA) are 2.5, 2.8, and 3.1 V for the 8000, 2000, and 800 ppm BDD electrodes, respectively. For comparison, the electrochemical window presented for a BDD electrode with even lower boron content (300 ppm) was also included in Fig. 5. This lowly doped electrode also displays an electrochemical window of 3.1 V, but both the HER and OER have a slower response to the overpotential. Thus, when the doping level is high, the higher surface conductivity of the electrode is associated to the high concentration in boron sites that act as catalyst for these reactions, as concluded by Cai [42]. On the contrary, the lower concentration of boron-rich sites on the electrode surface (e.g. the 300 ppm BDD electrode) blocks both the hydrogen and oxygen adsorption steps needed for the gas evolution reactions.

At this point, aiming to maximize the beneficial effects of cathodic pretreatments [1, 4] while minimizing the physical degradation of the BDD surface, a determination of the minimum (optimum) cathodic pretreatment was carried out. This was carried out using EIS measurements.

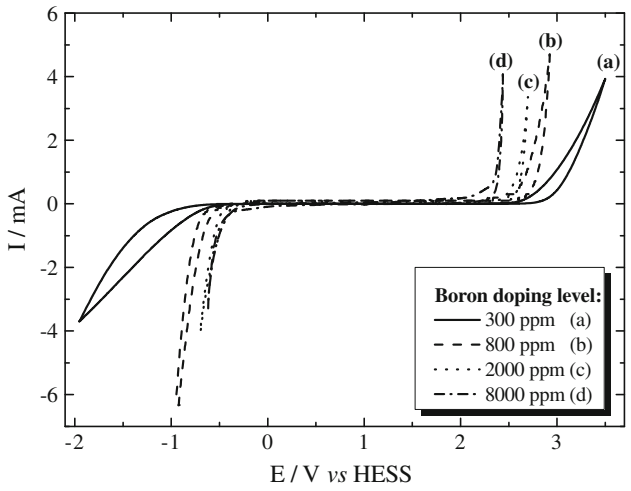

Fig. 5 Effect of the boron doping level on the electrochemical potential window presented by different as-received BDD electrodes in a 0.5 mol L^{-1} H_2SO_4 aqueous solution (v = 100 mV s^{-1})

Thus, the minimum value of charge density passed during the pretreatment necessary to decrease the resistance (R) associated to a high-frequency element in the complex-plane plot was determined; R values similar to the one attained in our previous report [1] were looked for (i.e. ~4 Ω cm^2 after −3.0 V for 30 min). Moreover, this minimum pretreatment should lead to a totally reversible cyclic voltammetric response of the redox couple $Fe(CN)_6^{4-/3-}$ without producing any physical degradation of the electrode surface.

By analysing the complex-plane plots shown in Fig. 6a, it can be concluded that the charge transfer resistance (R_2) of the as-received 800 ppm BDD electrode is 82 Ω cm^2. This resistance increases almost 200 times after an anodic pretreatment (passage of 5 C cm^{-2}), but decreases more than 90% to ~6 Ω cm^2 after a cathodic pretreatment (passage of −9 C cm^{-2}). Furthermore, this quite mild cathodic pretreatment is already sufficient to produce a reversible cyclic voltammetric response of the $Fe(CN)_6^{4-/3-}$ redox couple (see Fig. 6b). Similarly, the value of R_2 obtained for a cathodically pretreated 8000 ppm BDD electrode is less than 1% of that observed on the anodically pretreated electrode (Fig. 7a). Again, the cathodic pretreatment leads to a reversible cyclic voltammetric response of the $Fe(CN)_6^{4-/3-}$ redox couple (Fig. 7b). Therefore, without a doubt −9 C cm^{-2} (applying −1 A cm^{-2}) can be considered a minimum or optimum value of the cathodic charge density necessary to obtain high-quality electrochemical results (very conductive surface and high rate transfer for the $Fe(CN)_6^{4-/3-}$ redox couple) without producing any appreciable degradation of the BDD surfaces by the cathodic pretreatment. It should be mentioned that 2000 ppm BDD electrodes displayed behaviours similar to those shown in Figs. 6 and 7 for 800 and 8000 ppm BDD electrodes, respectively.

The values for the potential difference between the anodic and cathodic peaks (ΔE_p) listed in Table 1 show that the use of as-received BDD electrodes lead to quasi-reversible responses for the $Fe(CN)_6^{4-/3-}$ redox couple, probably due to remaining superficial H-terminations that were produced during the diamond deposition in the CVD chamber. Notwithstanding, these responses become irreversible after the mild anodic pretreatment, with a clear dependence on the boron-doping level of the electrode. However, after the cathodic pretreatment the behaviour becomes increasingly reversible with the boron doping level.

Liao et al. [46], using elastic recoil detection analysis showed that the superficial hydrogen concentration on BDD electrodes increases with the boron doping level. In this sense, Lombardi et al. [47] using theoretical calculations concluded that hydrogen bonding to boron is energetically favourable in diamond. Therefore, electrodes with

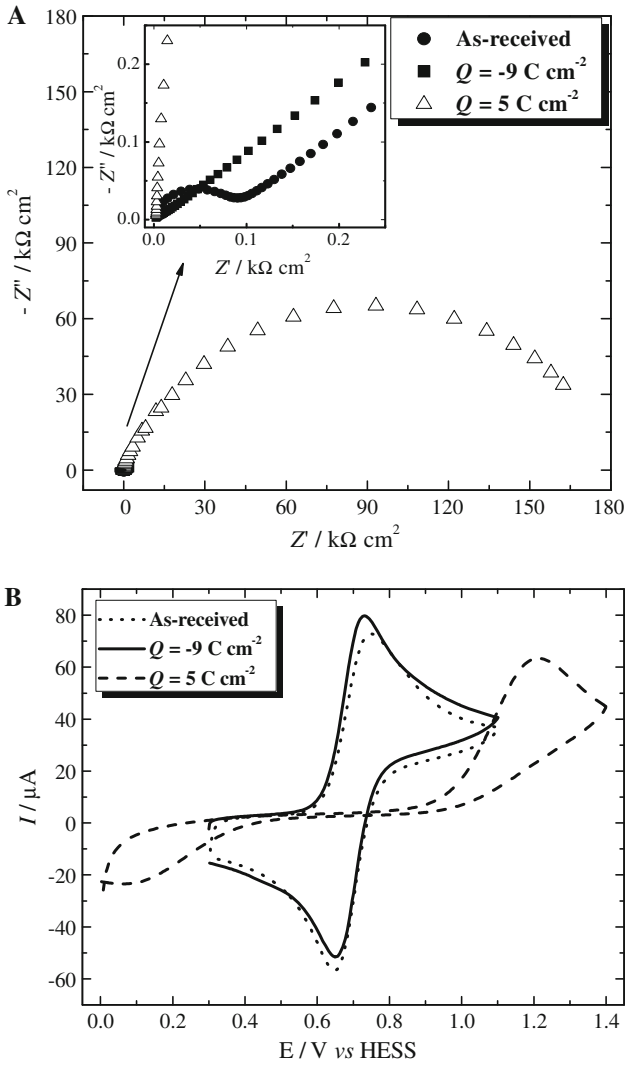

Fig. 6 **a** Complex-plane plots for an 800 ppm BDD electrode in a 1.0 mmol L^{-1} $K_4[Fe(CN)_6]$ + 0.5 mol L^{-1} H_2SO_4 aqueous solution recorded at 0.7 V with an ac perturbation of 5 mV (rms), from 10 MHz to 100 kHz: *spheres* as-received, *squares* cathodically pretreated by passing −9 C cm^{-2} using −1 A cm^{-2}, and *open triangles* anodically pretreated by passing 5 C cm^{-2} using 1 A cm^{-2}, **b** cyclic voltammograms obtained in the same solution on the same electrodes: *dotted line* as-received, *solid line* cathodically pretreated, and *dashed line* anodically pretreated

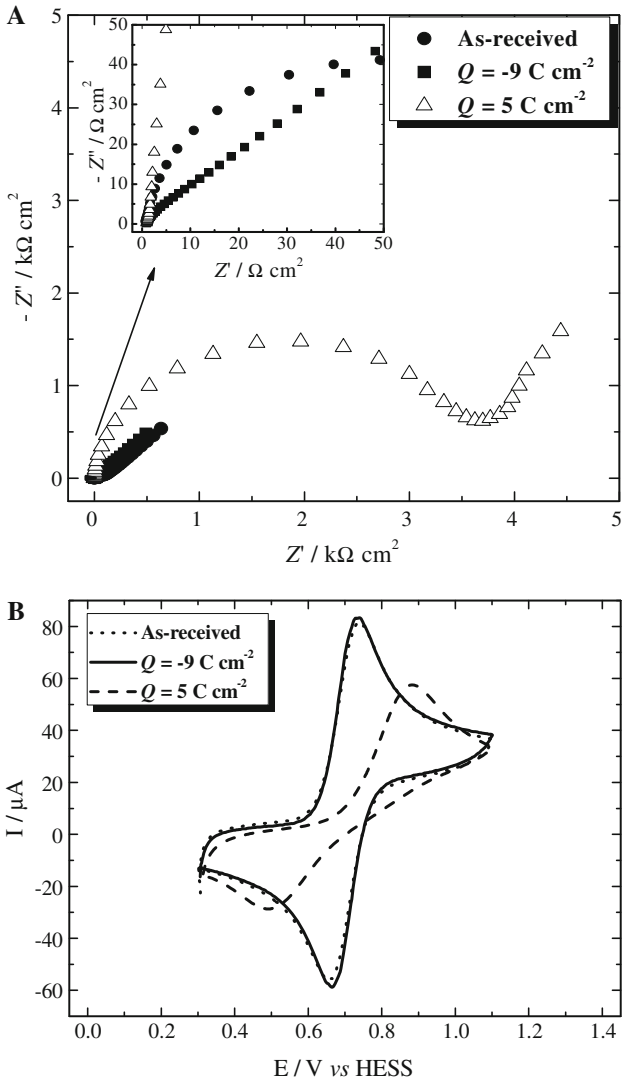

Fig. 7 **a** Complex-plane plots for an 8000 ppm BDD electrode in a 1.0 mmol L^{-1} $K_4[Fe(CN)_6]$ + 0.5 mol L^{-1} H_2SO_4 aqueous solution recorded at 0.7 V with an ac perturbation of 5 mV (rms), from 10 MHz to 100 kHz: *spheres* as-received, *squares* cathodically pretreated by passing −9 C cm^{-2} using −1 A cm^{-2}, and *open triangles* anodically pretreated by passing 5 C cm^{-2} using 1 A cm^{-2}, **b** cyclic voltammograms obtained in the same solution on the same electrodes: *dotted line* as-received, *solid line* cathodically pretreated, and *dashed line* anodically pretreated

high doping level and consequent higher boron content on their surfaces should present stronger superficial interactions with hydrogen than electrodes with low doping levels, as well as higher conductivity (rich in boron sites and H-terminated sites) [4]. These are quite plausible explanations for the better performance presented by the electrode with highest boron doping level, after the cathodic pretreatment, as shown in Table 1. Furthermore, the decrease in ΔE_p with the boron doping level is an additional indication of the plausibility of these explanations.

On the other hand, fitting the response of a proper electric equivalent circuit to the EIS data allows one to

Table 1 ΔE_p values related to the cyclic voltammograms for the $Fe(CN)_6^{3-/4-}$ redox couple (Figs. 6b, 7b), obtained using as-received (A-R) and anodically (positive charge density) or cathodically (negative charge density) pretreated 800, 2000, and 8000 ppm BDD electrodes

q (C cm^{-2})	ΔE_p (mV)		
	800 ppm	2000 ppm	8000 ppm
0 (A-R)	93	63	75
5	458	371	240
−9	69	63	61

obtain values for the characteristic parameters associated to the electrode process [48]. Figure 8 shows the two equivalent circuits (EC) whose responses were fitted to the EIS data by using the software developed by Boukamp [49]; an additional resistance (R_3) had to be added to the EC (Fig. 8b) so its response could fit the EIS data obtained with the anodically pretreated 800 ppm BDD electrode. The elements in these ECs are: electrolyte resistance (R_1), charge transfer resistance (R_2), resistance associated to surface blockage (R_3), constant phase elements (CPE_1 and CPE_2), and diffusional element (W). Table 2 shows the values of the parameters obtained in the fitting of these ECs to the EIS data for the three electrodes, as-received or electrochemically pretreated; the quite low ($\leq 2 \times 10^{-3}$) relative values of the weighted sum of squares (χ^2) shown in this table are indicative of the good quality of the fittings.

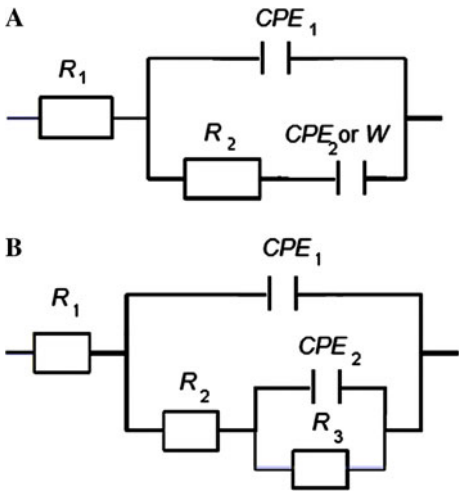

Fig. 8 Electric EC used for the fitting of the EIS spectra obtained for the $Fe(CN)_6^{3-/4-}$ redox couple using **a** BDD electrodes containing different boron doping levels, **b** anodically pretreated 800 ppm BDD electrode. See text

As it can be seen in Figs. 6a and 7a, the A-R BDD electrodes present an *RC* response at intermediate frequency values of the impedance spectra that is largely decreased after the cathodic pretreatment; however, this response becomes much more evident after the anodic pretreatment. This feature of the impedance response is also present in EIS data reported by other authors [29–31, 50]; Becker and Jüttner [29–31] postulated that the associated resistance could be explained by a partial blocking of the diamond electrode surface. Assuming that such is the case, then the anodic pretreatment (increment in oxygen-containing groups on the BDD surface) greatly augments this partial blocking and the cathodic pretreatment (increment in hydrogen-containing groups on the BDD surface) decreases it, as attested by the values of R_2 reported in Table 2. The significantly increased value of R_2 after the anodic pretreatment is indirectly observed by cyclic voltammetry (Figs. 6b, 7b), where an irreversible behaviour (Table 1) for the redox couple $Fe(CN)_6^{4-/3-}$ is clearly observed for all the electrodes.

Recently, Hernando et al. [51] reported EIS studies on ultrananocrystalline conductor diamond films (UNCD) modified by oxygen and hydrogen plasma treatments. The fitting of the experimental results was performed by means of a Randles circuit with a *CPE* to model the capacitive contribution of the interface. From the *CPE* parameters, these authors proposed that the interfacial impedance of oxygen-terminated UNCD is governed by sp^2-bonded carbon atoms in the grain boundaries, whereas the interfacial impedance of the hydrogen-terminated UNCD is determined by both the grain boundaries and the surface conductive hydrogen-terminated grains. Note that the BDD electrodes used in the present study do not present significant amounts of sp^2-bonded carbon atoms [4], contrary to

Table 2 Values for the elements of the EC shown in Fig. 8 obtained by adjusting their responses to the correspondent electrochemical impedance spectra (Figs. 6a, 7a) using the nonlinear least squares method [49]

q (C cm^{-2})	B content (ppm)	R_1 (Ω cm^2)	CPE_1 (μF cm^{-2} s^{n-1})	n_1	R_2 (Ω cm^2)	W (mF cm^{-2} s)	CPE_2 (mF cm^{-2} s^{n-1})	n_2	R_3 (kΩ cm^2)	χ^2
0 (A-R)	800	0.8	4.04	0.93	82.1	–	2.17	0.48	–	3.6×10^{-4}
	2000	0.8	0.11	0.91	23.5	2.07	–	–	–	5.7×10^{-4}
	8000	1.0	5.08	0.91	131.7	1.02	–	–	–	7.4×10^{-4}
5	800	2.2	3.80	0.97	16.7×10^3	–	7.52	0.67	175	5.4×10^{-4}
	2000	0.6	6.62	0.95	3.6×10^3	0.98	–	–	–	7.7×10^{-4}
	8000	1.1	9.04	0.74	3.3×10^3	1.87	–	–	–	1.2×10^{-3}
−9	800	1.1	8.78	0.95	6.55	–	1.76	0.47	–	2.9×10^{-5}
	2000	1.9	18.6	0.92	8.26	1.63	–	–	–	6.1×10^{-4}
	8000	0.9	71.0	0.77	22.7	1.21	–	–	–	1.8×10^{-3}

the UNCD films of the study reported by Hernando et al. [51].

As mentioned before, an additional circuit element (resistance R_3) had to be added to the EC (Fig. 8b) for the fitting of the impedance data for the anodically pretreated 800 ppm BDD electrode. The necessity of this extra resistance indicates that, in this specific case, the blocking of the electrode surface [29–31] is heterogeneous, with some sites with lower electrochemical activity and others that block redox reactions. Different types of conducting regions on BDD were previously reported [28, 32], as already reviewed. Holt et al. [28], based on CP-AFM and SECM images, concluded that the BDD films consisted of predominantly insulating, non-electrochemically active areas containing isolated sites of very high conductivity and electrochemical activity; they also found that at low doping levels the diamond surface only has limited sites ($\sim$10–60% of the geometric area) where electrochemistry can take place. Wilson et al. [32], using both C-AFM and CL imaging techniques, found two very different conductivity domains on oxygen-terminated BDD, caused by non-uniform boron uptake across the surface.

4 Conclusions

The physical degradation of an 800 ppm BDD surface after repeated cathodic pretreatments was evidenced using AFM and SEM measurements. The galvanostatic cathodic pretreatment in steps of -600 C cm^{-2} passed using -1 A cm^{-2} until -14000 C cm^{-2} caused an expressive physical degradation of the BDD surface, with film detachment (void formation) in some areas. As a consequence, a large increase in the electrocatalytic activity for the HER in acid media was observed in the Tafel plots. An increase in the highly conductive fraction of the BDD electrode surface is probably one of the consequences of this erosion phenomenon, since more boron-rich sites are exposed. Besides, the results obtained in the Tafel plots showed that the electrochemically active sites are largely dependent on the doping level.

Finally, comparison studies between cathodic pretreatments and an anodic pretreatment (using 5 C cm^{-2}) were done using EIS and cyclic voltammetry. The obtained results showed that an optimum value of the cathodic charge density needed to activate the BDD electrodes studied (800, 2000, and 8000 ppm of boron doping) is -9 C cm^{-2} (at -1 A cm^{-2}), without producing any observable physical degradation of the surface; then these electrodes present a reversible cyclic voltammetric response for the $Fe(CN)_6^{4-/3-}$couple. Consequently, whenever warranted, this is a recommended manner to activate BDD surfaces while avoiding unwanted degradation of the material. On the contrary, the anodically pretreated electrodes present irreversible cyclic voltammetric response for the $Fe(CN)_6^{4-/3-}$couple; this behaviour seems to be due to partial blocking of their surfaces caused by the introduction of oxygen terminations.

Acknowledgements The authors thank the Brazilian funding agencies CNPq, CAPES, and FAPESP for scholarships and financial support of this work.

References

1. Suffredini HB, Pedrosa VA, Codognoto L, Machado SAS, Rocha-Filho RC, Avaca LA (2004) Electrochim Acta 49:4021
2. Mahé E, Devilliers D, Comminellis Ch (2005) Electrochim Acta 50:2263
3. Holt KB, Sabin G, Compton RG, Foord JS, Marken F (2002) Electroanalysis 14:797
4. Salazar-Banda GR, Andrade LS, Nascente PAP, Pizani PS, Rocha-Filho RC, Avaca LA (2006) Electrochim Acta 51:4612
5. Codognoto L, Zuin VG, de Souza D, Yariwake JH, Machado SAS, Avaca LA (2004) Microchem J 77:177
6. Pedrosa VA, Codognoto L, Machado SAS, Avaca LA (2004) J Electroanal Chem 573:11
7. Pedrosa VA, Suffredini HB, Codognoto L, Tanimoto ST, Machado SAS, Avaca LA (2005) Anal Lett 38:1115
8. Oliveira RTS, Salazar-Banda GR, Ferreira VS, Oliveira SC, Avaca LA (2007) Electroanalysis 19:1189
9. Garbellini GS, Salazar-Banda GR, Avaca LA (2007) J Braz Chem Soc 18:1095
10. Medeiros RA, Carvalho AE, Rocha-Filho RC, Fatibello-Filho O (2007) Anal Lett 40:3195
11. Oliveira RTS, Salazar-Banda GR, Avaca LA (2008) Electroanalysis 20:396
12. Medeiros RA, Carvalho AE, Rocha-Filho RC, Fatibello-Filho O (2008) Quim Nova 31:1405
13. Medeiros RA, Carvalho AE, Rocha-Filho RC, Fatibello-Filho O (2008) Talanta 76:685
14. Garbellini GS, Salazar-Banda GR, Avaca LA (2009) Food Chem 16:1029
15. Sartori ER, Medeiros RA, Rocha-Filho RC, Fatibello-Filho O (2009) J Braz Chem Soc 20:360
16. Lourenção BC, Medeiros RA, Rocha-Filho RC, Mazo LH, Fatibello-Filho O (2009) Talanta 78:748
17. Andrade LS, Rocha-Filho RC, Cass QB, Fatibello-Filho O (2009) Electroanalysis 12:1475
18. Batista EF, Sartori ER, Medeiros RA, Rocha-Filho RC, Fatibello-Filho O (2010) Anal Lett 43:1046
19. Lévy-Clement C, Ndao NA, Katty A, Bernard M, Deneuville A, Comninellis C, Fujishima A (2003) Diam Relat Mater 12:606
20. Bouamrane F, Tadjeddine A, Butler JE, Tenne R, Levy-Clement C (1996) J Electroanal Chem 405:95
21. Ndao NA, Zenia F, Deneuville A, Bernard M, Levy-Clement C (2000) Diam Relat Mater 9:1175
22. Sine G, Ouattara L, Panizza M, Ch Comninellis (2003) Electrochem Solid State Lett 6:D9
23. Deuerler F, Lemmer O, Frank M, Pohl M, Hessing C (2002) Int J Refract Met Hard Mater 20:115
24. Bregliozzi G, Haenni W, Haefke H (2004) J Mater Sci 39:6603
25. Katsuki N, Takahashi E, Toyoda M, Kurosu T, Iida M, Wakita S, Nishiki Y, Shimamune T (1998) J Electrochem Soc 145:2358
26. Panizza M, Siné G, Duo I, Quattara L, Comninellis C (2003) Electrochem Solid State Lett 6:D17

27. Duo I, Levy-Clement C, Fujishima A, Comninellis C (2004) J Appl Electrochem 34:935
28. Holt KB, Bard AJ, Show Y, Swain GM (2004) J Phys Chem B 108:15117
29. Becker D, Jüttner K (2003) J Appl Electrochem 33:959
30. Becker D, Jüttner K (2003) New Diam Front Carbon Technol 13:67
31. Becker D, Jüttner K (2003) Electrochim Acta 49:29
32. Wilson NR, Clewes SL, Newton ME, Unwin PR, Macpherson JV (2006) J Phys Chem B 110:5639
33. Szunerits S, Mermoux M, Crisci A, Marcus B, Bouvier P, Delabouglise D, Petit J-P, Janel S, Boukherroub R, Tay L (2006) J Phys Chem B 110:23888
34. Wang S, Swain GM (2007) J Phys Chem B 111:3986
35. Wheeler DW, Wood RJK (2003) Surf Eng 19:466
36. Carter TJ, Cornish LA (2001) Eng Fail Anal 8:113
37. Wu TI, Wu JK (2002) Mater Lett 53:193
38. Perng TP, Wu JK (2003) Mater Lett 57:3437
39. Hagi H (1997) Mater Trans JIM 38:970
40. Eliaz N, Banks-Sills L, Ashkenazi D, Eliasi R (2004) Acta Mater 52:93
41. Suffredini HB, Machado SAS, Avaca LA (2004) J Braz Chem Soc 15:16
42. Cai Y (2005) PhD thesis, Cleveland. http://etd.ohiolink.edu/view.cgi?acc_num=case1120759456
43. Davies TJ, Moore RR, Banks CE, Compton RG (2004) J Electroanal Chem 574:123
44. Davies TJ, Banks CE, Compton RG (2005) J Solid State Electrochem 9:797
45. Davies TJ, Compton RG (2005) J Electroanal Chem 585:63
46. Liao C, Wang Y, Yang S (1999) Diam Relat Mater 8:1229
47. Lombardi EB, Mainwood A, Osuch K (2004) Phys Rev B 70:205201
48. Lasia A (1999) In: Conway BE, Bockris JO'M, White RE (eds) Modern aspects of electrochemistry, vol 32, chap 2. Kluwer Academic Press, Boston
49. Boukamp BA (1986) Solid State Ionic 18:136
50. Ferro S, De Battisti A (2002) Electrochim Acta 47:1641
51. Hernando J, Lud SQ, Bruno P, Dieter M, Gruen DI, Stutzmann M, Garrido JA (2009) Electrochim Acta 54:1909